Proceedings of the European Conference Physics of Magnetism 2011 (PM'11), Poznań, June 27–July 1, 2011

Magnetoresistance and Intrinsic Pinning of Vortices in the Untwinned $YBa_2Cu_3O_{7-\delta}$ Single Crystals with Optimal Oxygen Content and a Small Deviation from the Oxygen Stoichiometry

R.V. Vovk[a,*], V.M. Gvozdikov[a], M.A. Obolenskii[a], Z.F. Nazyrov[a] and V.V. Kruglyak[b]

[a]Kharkov National University, 4 Svoboda Sq., 61077 Kharkov, Ukraine

[b]University of Exeter, Stocker Road, Exeter, EX4 4QL, United Kingdom

We study the temperature dependence of the in-plane magnetoresistance $\rho_{ab}(T)$ in untwinned $YBa_2Cu_3O_{7-\delta}$ single crystals with the optimal oxygen content and with a small deficit of oxygen atoms at different angles between the external magnetic field 15 kOe and the ab-planes α. We found that at high temperatures in the pseudogap region external magnetic field does not affect the $\rho_{ab}(T)$ but it broadens transitional region $T_c - T_{c0}$ from 0.3 K at zero field and $\alpha = 0$ to approximately 6 K at $\alpha = 60^\circ$ in the field. In case of optimal doping the function $\rho_{ab}(T)$ display a 3D to 2D dimensional crossover when temperature decreases from T_c to T_{c0} and scaling near the T_{c0} which we relate to the flux-flow and vortex-lattice melting. In the underdoped sample the vortices are effectively pinned by the random oxygen vacancies and the function $\rho_{ab}(T)$ in transitional region has smooth tails without any traces of crossover and scaling.

PACS: 74.25.Fy, 74.25.Qt

1. Introduction

It is well known that external magnetic field influences the shape of the temperature behavior of the resistance of the high-T_c cuprates nearby the superconducting transition. The transitional region broadens and the magnetoresistance $\rho(T)$ acquires non-monotonous features which are attributed to the vortex dynamics. The latter is very complex in cuprates which are layered (quasi two-dimensional) strongly correlated non Fermi-liquid conductors with the pseudogap in their energy spectrum. The phase diagram of cuprates on the plane temperature–oxygen per Cu site includes the parabolic superconducting dome and the pseudogap crossover line above [1, 2]. In between there is a region of the Nernst-effect which is interpreted as a result of the vortices present well above the T_c. The nature of these vortices as well as the origin of the pseudogap is a matter of hot debates so far [2].

Contrary to the enigmatic normal properties the superconducting ones in cuprates are very much the same as in conventional layered superconductors. In particular, the Abrikosov vortices phenomenology is well understood [3]. The unconventional features in this phenomenology arise due to the very small atomic scale coherence length ξ and very large penetration depth λ which, in particular, makes oxygen vacancies [4] and atomic impurities [5, 6] effective pinning centers. Twins, grain boundaries, clusters of point defects also strongly pin vortices complicating thereby the exploration of the oxygen vacancies influence on the phase state of the vortex matter in cuprates. The layers as well produce the so called intrinsic pinning in the tilted magnetic fields.

To study the above points in a more detail we measured the temperature dependence of the in-plane resistance in untwinned $YBa_2Cu_3O_{7-\delta}$ single crystals with a small oxygen hypostoichiometry in the tilted at different angles α external magnetic field 15 kOe. The usage of untwinned single crystals excludes the influence of the grain and twin boundaries on the vortex pinning. The intrinsic pinning in our experiments vary by the tuning of the tilt angle α.

An important property of the $YBa_2Cu_3O_{7-\delta}$ compound is that one can relatively easily obtain a necessary concentration of the point defects by the variation of the oxygen content [5]. The resulting changes in the $\rho_{\alpha\beta}(T)$ makes it possible to study the correlations between the shape of the magnetoresistance and the concentration of the point defects. We analyze then these correlations in terms of the vortex matter near the transition temperature.

* corresponding author; e-mail: Ruslan.V.Vovk@univer.kharkov.ua

2. Experimental techniques

The $YBa_2Cu_3O_{7-\delta}$ single crystals were grown in a gold crucible with the solution-melting method, with the methodology described previously [5]. The $YBa_2Cu_3O_{7-\delta}$ oxygen saturating regime leads to the *tetra-ortho* structural transition that in its turn results to the crystal twinning in order to minimize its elastic energy. To obtain untwinned samples, we used a special cell at 420 °C and pressure 30–40 GPa, in accordance to the procedure of Giapintzakis et al. [7]. To obtain homogeneous oxygen content, the crystal was annealed again in an oxygen flow at a temperature of 420 °C for seven days.

To form electric contacts the standard four-contact scheme was used. In this, silver paste was applied onto the crystal surface and the connection of silver conductors (with diameter 0.05 mm). Thereafter, they were annealed at a temperature of 200 °C in an oxygen atmosphere for 3 h. This methodology results in contacts with resistance smaller than 1 Ω and allows measurements with a current of 10 mA in the ab-plane. All the measurements were performed in a temperature drift mode using the method for two opposite directions of the transport current. This effectively eliminates the impact of the parasitic signal. A platinum thermo-resistor was used to monitor the temperature, whereas the voltage was measured across the sample and the reference resistor with V2-38 nanovoltmeters. Here, the critical temperature (T_c) was defined as the temperature corresponding to the main maximum in the $d\rho_{ab}(T)/dT$ dependence in the superconductive transition similarly to previous studies [8]. To produce oxygen hypostoichiometric samples, the crystal was annealed in an oxygen flow, at a temperature of 650 °C for 48 h. The measurements were performed 7 days after annealing to avoid the influence of the relaxation effects. The magnetic field at 15 kOe was created by an electromagnet, which could vary the orientation of the field relative to the crystal. The accuracy of the field orientation relative to the sample was better than 0.2°. A bridge was mounted in the measuring cell so that the vector field H was always perpendicular to the vector of the transport current j.

3. The results of measurements

The temperature behavior of the in-plane magnetoresistance $\rho_{ab}(T)$ of the $YBa_2Cu_3O_{7-\delta}$ single crystals, measured at different tilt angles $\alpha \equiv \angle(\boldsymbol{H}, ab)$ between the applied external magnetic field $H = 15$ kOe and the basal ab-planes are shown in Fig. 1. Sample in Fig. 1a is optimally doped with the oxygen atoms so that its critical temperature T_c at zero field $H = 0$ (curve 1) is close to the maximal value of about 93 K at the apex of the superconductimg dome. Curves 2–9 were measured in external magnetic field $H = 15$ kOe at different tilt angles α from zero (curve 2) up to 90° (curve 9). All notations in Fig. 1b are the same as in Fig. 1a. The difference is in the oxygen content of the samples which in Fig. 1b is slightly smaller than the optimal value. That has two consequences. First, the critical temperature at $H = 0$ is slightly smaller (92 K) in Fig. 1b than in Fig. 1a where T_c is 93 K. Second, the shape of the curves 2–9 nearby the critical temperature are dramatically different which is more clear seen in Fig. 2 displaying the temperature derivatives of the magnetoresistance nearby T_c. The high temperature linear asymptotes $\rho_0 = (A+BT)$ are slightly different in Fig. 1a and b but the temperature $T^* \approx 134$ K where all curves merge with this asymptotes remains approximately the same. This temperature demarcates the pseudogap regime $T \gg T^*$ from the one in which all curves $\rho_{ab}(T)$ go down up to the same temperature near T_c where they split into a fan at different tilt angles α. Figure 2a and b demonstrate clearly the difference: sharp peaks in the end of transition in the optimally doped samples and broad peak in the underdoped single crystals. In both cases external magnetic field broadens the transition region. It is more convenient to analyze the transitional region in terms of the conductivity $\sigma = \rho^{-1}(T)$.

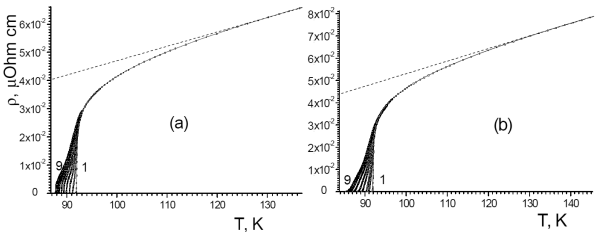

Fig. 1. Temperature dependence of the magnetoresistance $\rho_{ab}(T)$ measured in a single crystal $YBa_2Cu_3O_{7-\delta}$ with the optimal (a) and slightly decreased (b) oxygen content. The curves correspond to $H = 0$ (1) and $H = 15$ kOe at tilt angles $\alpha \equiv \angle(\boldsymbol{H}, ab)$: 0; 5; 10; 20; 30; 45; 60 and 90° (curves 2–9). The dashed lines display an extrapolation of the linear resistance in the pseudogap regions.

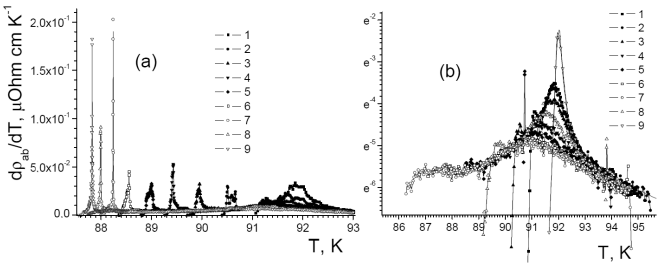

Fig. 2. Resistive transitions into the superconducting state in single crystals $YBa_2Cu_3O_{7-\delta}$ in the coordinates $d\rho_{ab}/dT - T$. The notations of the curves are the same as in Fig. 1.

Assuming that a deviation from the pseudogap asymptote $\sigma_0 = (A + BT)^{-1}$ near the critical temperature can be written as $\Delta\sigma = \sigma - \sigma_0 \sim (T - T_c)^{-\beta}$, we plot in Fig. 3 the inverse logarithmic derivative $\chi(T) = -d\ln\Delta\sigma/dT = \beta/(T - T_c)$ at the same tilt angles of the magnetic field α as in Figs. 1 and 2. A typical

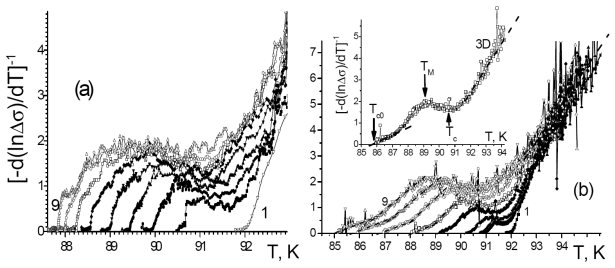

Fig. 3. Resistive transitions into the superconducting state in the optimally doped single crystals $YBa_2Cu_3O_{7-\delta}$ in the coordinates $\left[\frac{-\mathrm{d}(\ln\Delta\sigma)}{\mathrm{d}T}\right]^{-1} - T$. The notations of the curves are the same as in Fig. 1. The inset displays the curve obtained at $\alpha = 60°$. The dashed lines correspond to the asymptotes and the arrows mark the characteristic temperatures corresponding to the beginning, T_c, and the end of the superconducting transition T_{c0}. The T_M is a vortex-lattice melting temperature at which the kink has a maximum.

curve is shown in the inset in Fig. 3 from which one can see that the function $\chi(T)^{-1}$ has two asymptotes $\chi(T)^{-1} = \beta_{c0}^{-1}(T - T_{c0})$ and $\chi(T)^{-1} = \beta_c^{-1}(T - T_c)$ at temperatures T_c and T_{c0}. In this, T_{c0} is the critical temperature of the transition in para-coherent area, determined at the point of intersection with the linear interval, approximating the so-called para-coherent area with the axis of temperature. T_c is the temperature corresponding to the mean-field critical temperature, determined as the maximum in the curves $\mathrm{d}\rho_{ab}(T)/\mathrm{d}T$ [8]. Between these asymptotes at the temperature T_M there is a kink which shifts towards lower temperatures and enhances its height and width with the enhancement of the tilt angle α.

4. Outlook and conclusions

Analyzing the resistive measurements in cuprates above the critical temperature in external magnetic field one has to keep in mind that despite the nearly 25 years of intensive researches neither the nature of the charge carriers nor the mechanisms of the conductivity in cuprates are not known at the moment. Recent observation of the quantum magnetic oscillations in the underdoped cuprates [9–11] revealed two types of the fermion-type carriers, negatively charged "electrons" and positively charged "holes". The phase diagram of cuprates in the region of the hole concentration of our experiments $p < 0.16$ consists of the parabolic superconducting dome $T_c = T_c^{\max}[1 - 82.6(0.16 - p)^2]$ and a pseudogap crossover line $\Delta_{pg} = \Delta_{pg}^{\max}(0.27 - p)/0.22$ above it. Here p stands for a hole concentration per cuprum atom [1]. In the space between the pseudogap and the dome, at hole concentration $p < 0.16$, the Nernst effect holds which most likely is related to the vortices of unknown nature which in some theories are related to the gauge fields of the 2D strongly correlated charge carriers of cuprates [2].

The pseudogap regime is characterized by the linear temperature resistance $\rho_0 = A + BT = \sigma_0^{-1}$ at $T > T^*$. This regime is seen clear in Fig. 1. Although below the T^* the resistance curve in Fig. 1 bends down we cannot attribute this only to the beginning of the superconducting transition since it is well known that for smaller p the resistance curve $\rho(T)$ in underdoped cuprates first upturns above ρ_0 before transition to the superconducting state at critical temperature [4]. The physics behind this behavior is unclear so far as well as many other normal properties of cuprates.

On the other hand, the superconducting properties of cuprates are more or less the same as in conventional superconductors. Because of that we can make some conclusions concerning the physics in transitional region nearby the critical temperature shown in Figs. 2 and 3. The broadening of the resistance in that region in external magnetic field is caused mainly by the Abrikosov vortices. Without magnetic field the width of transition is small $\Delta T_c \approx 0.3$ K. In external magnetic field in the optimally doped samples it enhances gradually up to the value $\Delta T_c \approx 7$ K at $\alpha = 90°$ as one can see in Fig. 3b. The function $\chi(T)$ in that figure has two linear asymptotes $\chi(T)^{-1} = \beta_{c0}^{-1}(T - T_{c0})$ and $\chi(T)^{-1} = \beta_c^{-1}(T - T_c)$ nearby the T_{c0} and T_c with $\beta_c \approx 1$ and $\beta_{c0} \approx 1/2$ which means a crossover from one regime to another when temperature decreases from T_c to T_{c0}. We argue below that this crossover can be related to the well known 3D to 2D crossover in the upper critical field $H_{c2}(T)$ since the ratio $H/H_{c2}(T)$ determines both the flux-flow resistance $\rho_{ff}(T) = \rho H/H_{c2}(T)$ and the Abrikosov lattice elastic moduli $c_{ij} = c_{ij}[H/H_{c2}(T)]$, which are polynomials of this ratio [12]. It is well known that in layered superconductors in a tilted magnetic field the function $H_{c2}(T)$ displays a 3D to 2D-dimensional crossover [13]. This crossover is a smooth transition from the linear dependence $H_{c2}(T) \propto (T - T_c)$ just below T_c, typical for the 3D samples, to the square root dependence $H_{c2}(T) \propto (T - T_{c0})^{1/2}$ which holds in 2D thin layers. A nontrivial feature of this 3D to 2D crossover is that the temperature T_{c0} is lower than the T_c. As was shown in the papers [14, 15] the difference $T_c - T_{c0}$ depends on the strength and some other details of the coupling between the layers.

The resistance $\rho_{ab}(T) = \rho_0(1 + \Delta\sigma\rho_0)^{-1}$ near the transition is determined by the term $\Delta\sigma\rho_0$ which means that singularities in the $\rho_{ab}(T)$ are of the same nature as in the $\Delta\sigma(T)$. (In case $\Delta\sigma\rho_0 \ll 1$ the quantity $\Delta\rho_{ab} = \rho_{ab} - \rho_0$ can be written as $\Delta\rho_{ab} \approx -\rho_0^2\Delta\sigma$.)

In optimally doped untwinned single crystals there are no pinning centers which may fix or distort the Abrikosov lattice. Under such circumstances it is naturally to assume that the resistance near the transition temperature in our experiments is due to the flux-flow mechanism whose contribution to the $\rho_{ab}(T)$ is given by the formula $\rho_{ff}(T, \alpha) = \rho H^{\mathrm{perp}}(\alpha)/H_{c2}(T)$. For fixed tilt angle α the value of $H^{\mathrm{perp}}(\alpha)$ is constant and the temperature behavior of the flux-flow resistance completely depends on the $H_{c2}(T)$ which grows up and displays 3D to 2D crossover with the decrease of temperature. Therefore the $\rho_{ff}(T, \alpha)$ decreases as a function of temperature and

displays near the superconducting transition the same 3D to 2D crossover as that observed in the function $\Delta\sigma(T)$. Approximating the value of the resistance decrease near the transition $|\Delta\rho_{ab}| \approx \Delta\sigma\rho_0^2$ by the flux-flow resistance $\rho_{\rm ff}(T,\alpha)$ we can explain the crossover in $\Delta\sigma(T)$ and related asymptotes $\chi(T)^{-1} = \beta_{\rm c0}^{-1}(T - T_{\rm c0})$ and $\chi(T)^{-1} = \beta_{\rm c}^{-1}(T - T_{\rm c})$ by the 3D to 2D crossover in the upper critical field $H_{\rm c2}(T)$ and in the $\rho_{\rm ff}(T,\alpha)$. With the enhancement of the tilt angle α a perpendicular to layers component of the external magnetic field $H^{\rm perp}(\alpha)$ and $\rho_{\rm ff}(T,\alpha)$ increase in agreement with our observations. The kink between the asymptotes is related to the transitional region of the 3D to 2D crossover. This crossover through the elastic moduli of the Abrikosov lattice $c_{ij} = c_{ij}[H/H_{\rm c2}(T)]$ has also an impact on the melting line [16, 17]. The melting line $H_{\rm M}(T)$ goes below the $H_{\rm c2}(T)$ on the phase diagram and in the absence of the pinning centers depends on the shape of the $H_{\rm c2}(T)$. The flux-flow resistance of the melted and regular Abrikosov lattices are different. The melted Abrikosov lattice is in a disordered glassy state for which, as was shown in [6], the function $\chi(T)$ must display a scaling in some reduced coordinates. The corresponding plot is given in Fig. 4. It really displays a scaling close to the temperature $T_{\rm c0}$.

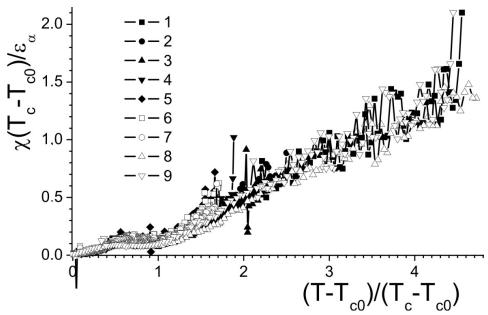

Fig. 4. Resistive transitions into the superconducting state in the optimally doped single crystals $YBa_2Cu_3O_{7-\delta}$ in the reduced coordinates $\chi(T_c - T_{c0})/\varepsilon_\alpha - (T - T_{c0})/(T_c - T_{c0})$. The notations of the curves are the same as in Fig. 1, where $\varepsilon_\alpha = (\sin^2\alpha + \varepsilon^2\cos^2\alpha)^{1/2}$ and the anisotropy $\varepsilon = 6{-}9$.

Deviation from the optimal doping towards the underdoped region $p < 0.16$ brings oxygen vacancies into the ab-planes which are effective pinning centers in cuprates. A pinned Abrikosov lattices is distorted and does not flow. The resistance in that case is due to the hopping of the vortices and 3D to 2D crossover is absent. That explains a dramatic difference between the pictures in Fig. 2a and b.

In conclusion, we found that in optimally doped untwinned single crystals YBaCuO: (i) the function $\chi(T)$ has linear asymptotes $\chi(T)^{-1} = \beta_{\rm c0}^{-1}(T - T_{\rm c0})$ and $\chi(T)^{-1} = \beta_{\rm c}^{-1}(T - T_{\rm c})$ nearby the $T_{\rm c0}$ and $T_{\rm c}$ with $\beta_{\rm c} \approx 1$ and $\beta_{\rm c0} \approx 1/2$. (ii) We relate this with the well known 3D to 2D crossover in the upper critical field $H_{\rm c2}(T)$ in the layered superconductors which through the ratio $H/H_{\rm c2}(T)$ influences the flux-flow resistance and the melting line of the Abrikosov vortex-lattice. (iii) The width of transitional region $T_{\rm c} - T_{\rm c0}$ increases from 0.3 K at zero field and $\alpha = 0$ to approximately 6 K at $\alpha = 60°$. (iv) The function $\chi(T)$ displays a universal scaling near the temperature $T_{\rm c0}$ which means a melting of the Abrikosov vortex-lattice. (v) All these features are absent in the samples with a small deviation from the oxygen stoichiometry in which oxygen vacancies effectively pin the vortices making impossible the mechanisms of resistance discussed above in points (i)–(iv).

Acknowledgments

This work was supported in part by European Commission CORDIS Seven Framework Program, project No. 247556.

References

[1] S. Hufner, M.A. Hossail, A. Domascelli, G.A. Sawatsky, *Rep. Prog. Phys.* **71**, 062501 (2008).

[2] P.A. Lee, N. Nagaosa, X.G. Wen, *Rev. Mod. Phys.* **78**, 17 (2006).

[3] G. Blatter, M.V. Feigel'man, V.B. Geshkenbein, A.I. Larkin, V.M. Vinokur, *Rev. Mod. Phys.* **66**, 1125 (1994).

[4] A.A. Zavgorodniy, R.V. Vovk, M.A. Obolenskii, A.V. Samoilov, *Low Temp. Phys.* **36**, 143 (2010).

[5] R.V. Vovk, M.A. Obolenskii, A.V. Bondarenko, I.L. Goulatis, A.V. Samoilov, A. Chroneos, V.M. Pinto Simoes, *J. Alloys Comp.* **464**, 58 (2008).

[6] R.M. Costa, I.C. Riegel, A.R. Jurelo, J.L. Pimentel Jr., *J. Magn. Magn. Mater.* **320**, 493 (2008).

[7] J. Giapintzakis, D.M. Ginzberg, P.D. Han, *J. Low Temp. Phys.* **77**, 155 (1989).

[8] L. Mendonca Ferreira, P. Pureur, H.A. Borges, P. Lejay, *Phys. Rev. B* **69**, 212505 (2004).

[9] N. Doiron-Leyraud, C. Proust, D. LeBoeuf, J. Levallois, J.-B. Bonnemaison, R. Liang, D.A. Bonn, W.N. Hardy, L. Taillefer, *Nature* **447**, 565 (2007).

[10] R. Daou, N. Doiron-Leyraud, D. LeBoeuf, S.Y. Li, F. Laliberté, O. Cyr-Choinière, Y.J. Jo, L. Balicas, J.-Q. Yan, J.-S. Zhou, J.B. Goodenough, L. Taillefer, *Nature Phys.* **5**, 31 (2009).

[11] F. Rullier-Albenque, H. Alloul, F. Balakirev, C. Proust, *Eur. Phys. Lett.* **81**, 37008 (2008).

[12] E.H. Brandt, *Phys. Rev. B* **34**, 6514 (1986); **71**, 014521 (2005).

[13] B.Y. Jin, J.B. Ketterson, *Adv. Phys.* **38**, 189 (1989).

[14] V.M. Gvozdikov, *Low Temp. Phys.* **16**, 1 (1990).

[15] V.M. Gvozdikov, M. Teixeira, *Low Temp. Phys.* **19**, 1302 (1993).

[16] V.M. Gvozdikov, L.Z. Kaganovsky, *Czechoslovak J. Phys.* **46**, S3, 1181 (1996).

[17] V.M. Gvozdikov, M. Teixeira, *Proc. Kharkov Nat. University* **476**, 42 (2000).